Multicomponent Monolayer Architectures at the Solid–Liquid Interface: Towards Controlled Space-Confined Properties and Reactivity of Functional Building Blocks**

Mathieu Surin and Paolo Samorì

*A*chieving full, nanometer-scale control over the positioning and organization of molecules into monolayers at surfaces represents a major challenge, with potential interest in the field of fabrication of multifunctional nanodevices.[1] Bottom-up approaches successfully exploit the self-assembly of molecules to generate preprogrammed structures and patterns on such a scale.[2–8] In this context, scanning tunneling microscopy (STM) is a tool of choice to characterize the molecular packing on solid surfaces and unravel dynamic processes such as organic monolayer formation, in particular at the solid–liquid interface.[9,10] While the formation of single-component self-assembled monolayers and their characterization by STM has been thoroughly reported for more than a decade,[11] only recently have interesting studies on multicomponent two-dimensional (2D) architectures been proposed. In this contribution we highlight various recent results based on novel approaches for the self-assembly of multicomponent 2D nanostructures at the solid–liquid interface and their characterization on the submolecular scale by in situ STM studies.

The controlled formation of ordered multicomponent nanostructures with a periodic structural motif is not trivial as most binary mixtures are prone to undergo phase segregation or to form randomly mixed domains.[12] Ordered bi- or multicomponent nanostructures can be formed by a subtle interplay between intramolecular, intermolecular, and interfacial interactions, and in particular by combining principles of supramolecular chemistry and interfacial chemistry. An important role is played by the solvent, not only in view of its different interactions with the molecules, but also in light of the possibility to coadsorb at surfaces.[13] For example, De Feyter and co-workers observed the coadsorption of solvent (1-octanol) molecules within a monolayer of an isophtalic acid derivative (the "studied" molecule) on highly oriented pyrolytic graphite (HOPG). They showed the exchange dynamics between 1-octanol solvent molecules and the isophtalic acid proceeds at the monolayer domain boundaries, leading to a rearrangement of a large part of the monolayer within a domain in a cooperative manner (see details in Ref. [14]). Such a result is in line with the findings of Padowitz and co-workers, who employed thioether molecules coadsorbed within an alkane monolayer as tracers to follow the rate of exchange (adsorption–desorption processes) and the specific molecular processes at grain boundaries.[15]

Recently, a few STM studies reported the construction of mixed donor–acceptor monolayers by applying a solution containing the two molecular systems to crystalline solid surfaces such as HOPG. In a seminal work, Rabe and co-workers studied the monolayer formation of a donor–acceptor model system, namely isophtalic acid and pyrazine derivatives, forming hydrogen-bonded 2D networks on graphite, and compared the structure with a 3D crystalline

[*] Dr. P. Samorì
Istituto per la Sintesi Organica e la Fotoreattività
Consiglio Nazionale delle Ricerche (C.N.R.)
via Gobetti 101, 40129 Bologna (Italy)
Fax: (+39) 051-6399844
E-mail: samori@isof.cnr.it

Dr. M. Surin, Dr. P. Samorì
Nanochemistry Laboratory
ISIS/CNRS UMR 7006
Université Louis Pasteur
8, allée Gaspard Monge, 67083 Strasbourg (France)

Dr. M. Surin
Chimie des Matériaux Nouveaux
Université de Mons-Hainaut
20, Place du Parc, 7000 Mons (Belgium)

packing.[16] Similarly, the concept of the H-bonded network has been exploited to form discrete oligothiophene assemblies[17] or 2D crystals of perylene bisimide with two different partners, and the authors have suggested strategies to immobilize the multicomponent system at the liquid–solid interface.[18] Therefore, these multicomponent methodologies are complementary to the classical "one-component" approach in which the donor and acceptor are covalently linked, forming dyads and multiads.[19–24]

Furthermore, the controlled co-deposition of two components was proven to be a viable approach to govern the orientation of a discotic system with respect to the basal plane of the graphite substrate: The interaction of a Zn–porphyrin derivative with 1,4-diaza[2,2,2]bicyclooctane (DABCO) or bipyridine can, for example, drive the self-assembly towards either an edge-on or a face-on packing of porphyrin discs at the graphite–solution interface.[25]

Recently, different groups have developed donor–acceptor complexes using macrocycles (as electron donors) that can encapsulate functional units as electron acceptors, such as fullerene (C_{60}). This approach represents a route to change the reactivity of functional building blocks or to study physicochemical aspects of spatially confined functional units, and then compare them with the properties of their bulk. One can self-assemble in solution the host–guest system and directly adsorb it onto surfaces using a one-step deposition. Following this strategy, calixarenes were employed to host C_{60} within a self-assembled monolayer on Au(111).[26] In contrast, two recent papers describe a two-step procedure: First, a 2D monolayer of macrocycles is physisorbed onto HOPG, then a solution containing C_{60} is applied to the surface, yielding the encapsulation of the fullerene within the macrocycle. Mena-Osteritz and Bauërle described the adsorption of C_{60} on a dodecathiophene macrocycle and showed that although the C_{60} would sterically fit within the macrocycle cavity, it spontaneously tends to adsorb onto the rims of the macrocycle (see Figure 1).[27] At a high coverage of C_{60}, they observed that only one C_{60} unit can be adsorbed per macrocycle. In an independent report,[28] different authors also observed that C_{60} adsorbs on the bithiophene moieties of a different macrocycle; altogether, these results suggest a relatively strong π-donor/π-acceptor interaction between the thiophene moieties and C_{60}. However, the latter report proposed that two C_{60} molecules can adsorb per macrocycle, which can be explained in light of the larger macrocycle diameter (and unit cell area) compared to the thiophene macrocycle described in Ref. [27]. As an alternative to macrocycles, supramolecular arrays generated from trimesic acid (TMA) derivatives can be employed to encapsulate C_{60}[29] or coronene derivatives.[30] In this case, the absence of a preferential weak interaction, such as the one between an electron acceptor and a donor moiety (as described in Refs. [27,28]), allowed the incorporation of the conjugated units in the central vacancy of the supramolecular array.

By exploiting oligo(phenylene ethynylene) (OPE), which is known to form highly ordered monolayers on graphite,[31] different self-assembly behavior has been obtained by co-depositing phthalocyanine derivatives with OPE at surfaces. While octakis(octyloxy) phthalocyanine (PcOC8) forms isolated domains adsorbed on graphite, which are segregated from the OPE crystals on the tens-of-nanometers scale, ordered adlayers of phthalocyanine derivatives adsorbed on top of a first OPE layer have been observed using praseodymium bis(phthalocyanine) (Pr-[(PcOC8)_2]).[32] Nevertheless, these architectures were characterized by a poor control over the stoichiometry of the different components within the monolayer. This control could be attained through a careful choice of the molar ratio of the two systems in the solution applied to the surface. Very recently, Wan and co-workers described the co-adsorption of OPE and coronene (COR): Depending on the molar ratio, alternate single and molecular pair rows on HOPG can be observed, see Figure 2.[12] The relationship between the molar ratio and the distribution is somehow unexpected: For instance, a 1:1 molar ratio gives a two-by-two distribution of COR (i.e., rows of COR pairs) while a 1:2 molar ratio gives a one-by-one distribution of COR (i.e.,
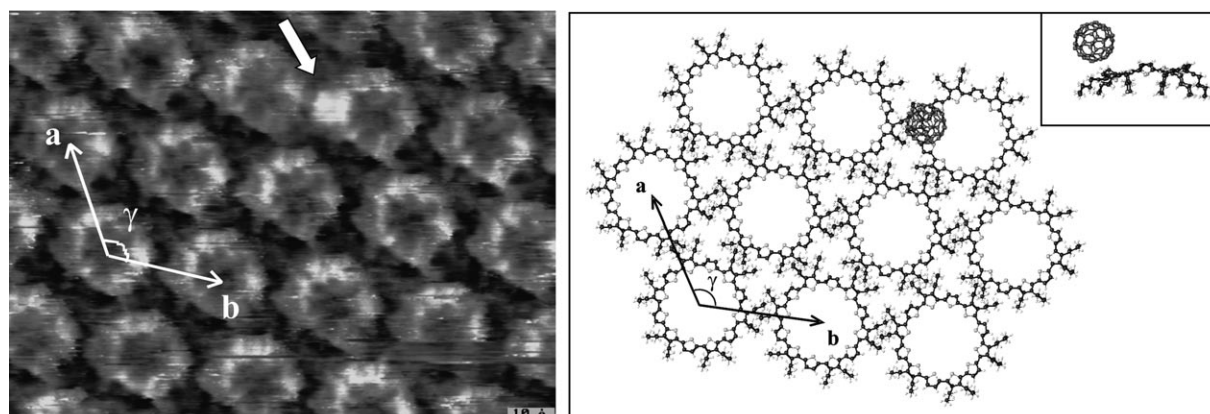
Figure 1. Left: STM image (11.6 nm × 8.7 nm) of a monolayer of a thiophene-based macrocycle on HOPG, including a complex with C_{60} (white arrow). Bias voltage $V = -700$ mV, average tunneling current $I = 44$ pA. Right: Calculated model of a closely packed monolayer of a macrocycle and a side view of the calculated energy-minimum conformation of the complex (inset, upper right). Reprinted with permission from Ref. [27].
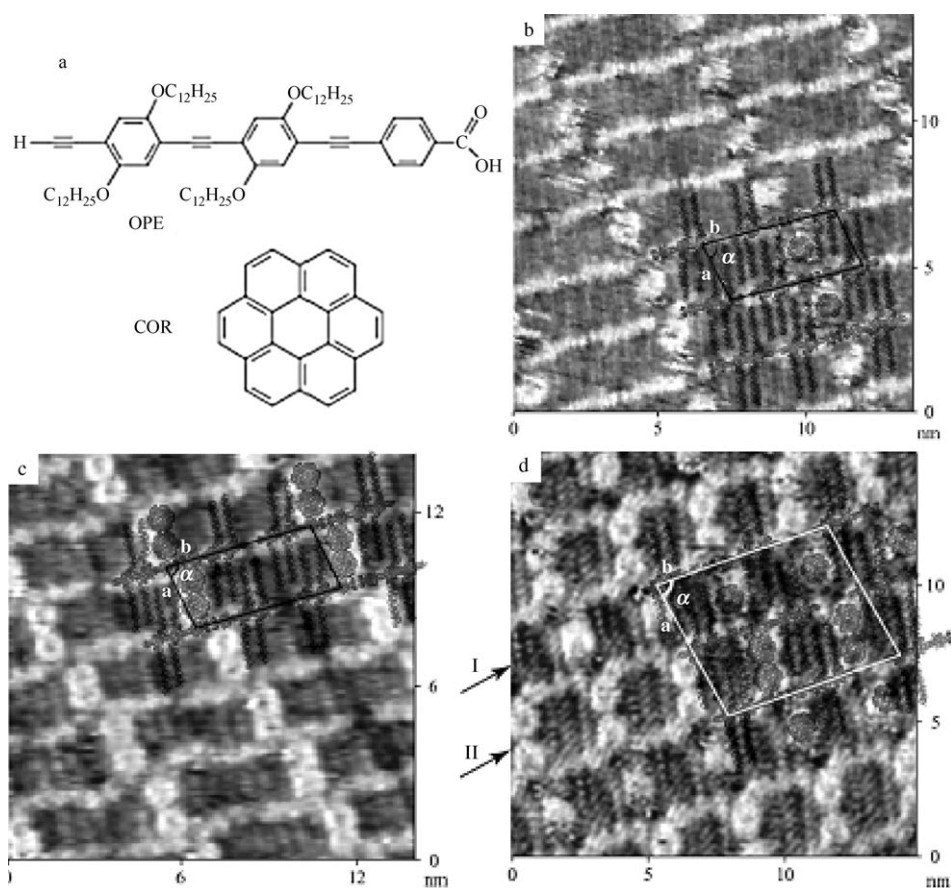
Figure 2. a) Chemical structures of OPE and COR; b) STM image of a one-by-one distribution (1:2 molar ratio of COR to OPE), $V = 874$ mV, $I = 498$ pA; c) STM image of a two-by-two distribution (1:1 molar ratio), $V = 759$ mV, $I = 735$ pA; d) STM image of a one-by-two distribution (3:2 molar ratio), $V = 920$ mV, $I = 652$ pA. Reprinted with permission from Ref. [12].

rows of single COR). The authors also describe the distribution of peptides in the OPE template, and in this case the dispersion of the peptide is controlled by the H-bonds with the terminal carboxylic groups of the oligomers. The structural model they propose consists of peptides that are arranged in pairs adsorbing only every two terminal carboxylic moieties of the OPE.

Charra et al. reported a similar approach, where a monolayer template was employed to control the positioning of functional units. They used a molecule consisting of a tristyrylbenzene core substituted with alkyl groups at the periphery. This system self-assembles into monolayers with a threefold symmetry on HOPG.[33] This assembly exposes "cavities" (i.e., uncovered HOPG) between the cores, dictated by the length of the alkyl groups, in which subsequently deposited guest molecules such as COR or hexabenzocoronene (HBC) can adsorb. Interestingly, by following the dynamics of the different guest molecules in situ at the liquid–solid interface and under vacuum, they showed that this monolayer template actually behaves like a "sieve"; guest molecules smaller than the channel width between two cavities (e.g., COR) can diffuse from cavity to cavity by a ther-

mally activated process, while larger molecules such as HBC remain sequestered in the cavity.

Rosei and co-workers proposed a method to control the molecular packing of TMA coadsorbed with a linear alcohol on HOPG. Due to the three carboxylic groups on the TMA unit, TMA forms H-bonds with the alcohol. When both components are mixed before imaging, two types of domains are observed in the monolayer on HOPG: a flowerlike pattern and a linear pattern. The former is the typical assembly of pure TMA in a threefold symmetry architecture, while the latter consists of a mixed monolayer made of TMA dimer tapes separated by a tape of perpendicular linear alcohol chains (1-heptadecanol in the case of Figure 3 b).[34] It is worth noticing that the authors ruled out the possibility of esterification between the two components. By changing the alcohol chain length, they were able to modulate the distance between TMA tapes. Interestingly, they found that all

alcohols with an odd number of carbon atoms produced a nearly perpendicular orientation of alcohol chain axis with respect to the TMA tape (see Figure 3 b), whereas they observed a tilted orientation for an even number of carbon atoms (see Figure 3 a). This difference is interpreted on the basis of the dense alkyl-chain packing in which adjacent chains are in a staggered arrangement: For even-numbered alcohols, efficient packing requires adjacent chains to shift by one carbon along the chain axis, resulting in the tilt of the chain with respect to the TMA tape.

Interestingly, STM at the solid–liquid interface has also proven to be a useful tool to study the self-assembly of nucleic acids. Very recently, Besenbacher and co-workers described the intermolecular H-bonding between pure and mixed assemblies of adenine and thymine physisorbed on HOPG.[35] As pointed out by the authors, it is indeed a great challenge to better understand the mechanism behind the assembly of DNA nucleobases in view of their potential complexation with proteins and with more complex biological systems.[35]

The exploration of multicomponent monolayer systems with STM is a rapidly evolving field, paving the route to-
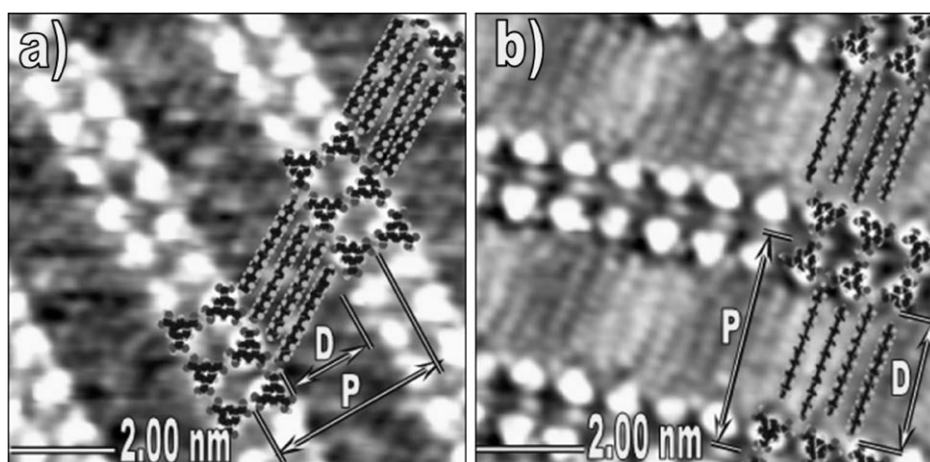
Figure 3. STM images of monolayers obtained by mixing TMA with a) 1-hexadecanol and b) 1-heptadecanol in heptanoic acid solution. Tunneling parameters: a) $V = -1.4$ V, $I = 200$ pA, and b) $V = -1.1$ V, $I = 200$ pA. Reprinted with permission from Ref. [34].

wards exciting applications in the realm of nanotechnology, for example, data storage and sensors. The studies highlighted in this paper show that various strategies can be undertaken towards a rational molecular nanopatterning of multicomponent architectures at surfaces, as a way to tune the reactivity of functional units or to study and exploit their space-confined properties. Furthermore, it represents the first step towards the formation of multifunctional 3D nanostructures. A precise self-assembly can be accomplished by tailoring specific and directional noncovalent interactions between molecules, by tuning parameters such as the molar ratio, solvent, and temperature, or by using templates to guide the positioning of specific molecules. To achieve a full control over the stoichiometry of multicomponent architectures, it will be of utmost importance to understand the complex thermodynamics governing the self-assembly process. Help in this regard could arise from molecular modeling as a route to unveil rational strategies for multicomponent molecular patterning at surfaces, and to single out the different energetic contributions governing the complex phenomena.

[1] See this special issue: *Adv. Mater.* **2006**, *18*, 1227–1329.
[2] P. Moriarty, *Rep. Prog. Phys.* **2001**, *64*, 297.
[3] See this special issue: *Science* **2002**, *295*, 2395–2433.
[4] S. Hecht, *Angew. Chem.* **2003**, *115*, 24; *Angew. Chem. Int. Ed.* **2003**, *42*, 24.
[5] F. Rosei, M. Schunack, Y. Naitoh, P. Jiang, A. Gourdon, E. Laegsgaard, I. Stensgaard, C. Joachim, F. Besenbacher, *Prog. Surf. Sci.* **2003**, *71*, 95.
[6] J. V. Barth, G. Costantini, K. Kern, *Nature* **2005**, *437*, 671.
[7] P. Samorì, V. Francke, K. Müllen, J. P. Rabe, *Chem. Eur. J.* **1999**, *5*, 2312.
[8] D. Bonifazi, H. Spillmann, A. Kiebele, M. de Wild, P. Seiler, F. Y. Cheng, H. J. Guntherodt, T. Jung, F. Diederich, *Angew. Chem.* **2004**, *116*, 4863; *Angew. Chem. Int. Ed.* **2004**, *43*, 4759.
[9] P. Samorì, *Scanning Probe Microscopies Beyond Imaging—Manipulation of Molecules and Nanostructures*, Wiley, Weinheim, **2006**.
[10] S. De Feyter, F. C. De Schryver, *J. Phys. Chem. B* **2005**, *109*, 4290.
[11] J. P. Rabe, S. Buchholz, *Science* **1991**, *253*, 424.
[12] J.-R. Gong, H.-J. Yan, Q.-H. Yuan, L.-P. Xu, Z.-S. Bo, L.-J. Wan, *J. Am. Chem. Soc.* **2006**, *128*, 12384.
[13] W. Mamdouh, H. Uji-i, J. S. Ladislaw, A. E. Dulcey, V. Percec, F. C. De Schryver, S. De Feyter, *J. Am. Chem. Soc.* **2006**, *128*, 317.
[14] A. Gesquière, M. M. Abdel-Mottaleb, S. De Feyter, F. C. De Schryver, M. Sieffert, K. Müllen, A. Calderone, R. Lazzaroni, J. L. Brédas, *Chem. Eur. J.* **2000**, *6*, 3739.
[15] D. F. Padowitz, D. M. Sada, E. L. Kemer, M. L. Dougan, W. A. Xue, *J. Phys. Chem. B* **2002**, *106*, 593.
[16] K. Eichhorst-Gerner, A. Stabel, G. Moessner, D. Declerq, S. Valiyaveettil, V. Enkelmann, K. Müllen, J. P. Rabe, *Angew. Chem.* **1996**, *108*, 1599; *Angew. Chem. Int. Ed. Engl.* **1996**, *35*, 1492.
[17] S. De Feyter, M. Larsson, N. Schuurmans, B. Verkuijl, G. Zoriniants, A. Gesquiere, M. M. Abdel-Mottaleb, J. van Esch, B. L. Feringa, J. van Stam, F. De Schryver, *Chem. Eur. J.* **2003**, *9*, 1198.
[18] S. De Feyter, A. Miura, S. Yao, Z. Chen, F. Würthner, P. Jonkheijm, A. P. H. J. Schenning, E. W. Meijer, F. C. De Schryver, *Nano Lett.* **2005**, *5*, 77.
[19] N. Tchebotareva, X. M. Yin, M. D. Watson, P. Samorì, J. P. Rabe, K. Müllen, *J. Am. Chem. Soc.* **2003**, *125*, 9734.
[20] P. Samorì, X. M. Yin, N. Tchebotareva, Z. H. Wang, T. Pakula, F. Jäckel, M. D. Watson, A. Venturini, K. Müllen, J. P. Rabe, *J. Am. Chem. Soc.* **2004**, *126*, 3567.
[21] P. Samorì, A. Fechtenkötter, E. Reuther, M. D. Watson, N. Severin, K. Müllen, J. P. Rabe, *Adv. Mater.* **2006**, *18*, 1317.
[22] A. Miura, Z. J. Chen, H. Uji-i, S. De Feyter, M. Zdanowska, P. Jonkheijm, A. P. H. J. Schenning, E. W. Meijer, F. Würthner, F. C. De Schryver, *J. Am. Chem. Soc.* **2003**, *125*, 14968.
[23] H. Uji-i, A. Miura, A. Schenning, E. W. Meijer, Z. J. Chen, F. Würthner, F. C. De Schryver, M. Van der Auweraer, S. De Feyter, *ChemPhysChem* **2005**, *6*, 2389.
[24] W. J. Shumate, D. L. Mattern, A. Jaiswal, D. A. Dixon, T. R. White, J. Burgess, A. Honciuc, R. M. Metzger, *J. Phys. Chem. B* **2006**, *110*, 11146.
[25] J. A. A. W. Elemans, M. C. Lensen, J. W. Gerritsen, H. van Kempen, S. Speller, R. J. M. Nolte, A. E. Rowan, *Adv. Mater.* **2003**, *15*, 2070.
[26] G. B. Pan, J. M. Liu, H. M. Zhang, L. J. Wan, Q. Y. Zheng, C. L. Bai, *Angew. Chem.* **2003**, *115*, 2853; *Angew. Chem. Int. Ed.* **2003**, *42*, 2747.
[27] E. Mena-Osteritz, P. Bauërle, *Adv. Mater.* **2006**, *18*, 447.
[28] G. B. Pan, X. H. Cheng, S. Höger, W. Freyland, *J. Am. Chem. Soc.* **2006**, *128*, 4218.
[29] S. J. H. Griessl, M. Lackinger, F. Jamitzky, T. Markert, M. Hietschold, W. M. Heckl, *J. Phys. Chem. B* **2004**, *108*, 11556.
[30] S. J. H. Griessl, M. Lackinger, F. Jamitzky, T. Markert, M. Hietschold, W. A. Heckl, *Langmuir* **2004**, *20*, 9403.
[31] P. Samorì, V. Francke, V. Enkelmann, K. Müllen, J. P. Rabe, *Chem. Mater.* **2003**, *15*, 1032.
[32] Z. Y. Yang, L. H. Gan, S. B. Lei, L. J. Wan, C. Wang, J. Z. Jiang, *J. Phys. Chem. B* **2005**, *109*, 19859.

[33] G. Schull, L. Douillard, C. Fiorini-Debuisschert, F. Charra, F. Mathevet, D. Kreher, A. J. Attias, *Nano Lett.* **2006**, *6*, 1360.

[34] K. G. Nath, O. Ivasenko, J. A. Miwa, H. Dang, J. D. Wuest, A. Nanci, D. F. Perepichka, F. Rosei, *J. Am. Chem. Soc.* **2006**, *128*, 4212.

[35] W. Mamdouh, M. Dong, S. Xu, E. Rauls, F. Besenbacher, *J. Am. Chem. Soc.* **2006**, *128*, 13 305.